Research Square

Preprints are preliminary reports that have not undergone peer review.
They should not be considered conclusive, used to inform clinical practice,
or referenced by the media as validated information.

Glue-Free Femtosecond Laser Welding of Polymer–Glass Interfaces for Lab-on-Chip Devices

Federica Torre

federica.torre@supsi.ch

University of Applied Sciences and Arts of Southern Switzerland

Matteo Porta

University of Applied Sciences and Arts of Southern Switzerland

Francesco Impaziente

University of Applied Sciences and Arts of Southern Switzerland

Anneke Orlandini

University of Applied Sciences and Arts of Southern Switzerland

Anna Valente

University of Applied Sciences and Arts of Southern Switzerland

Research Article

Keywords:

Posted Date: June 24th, 2026

DOI: https://doi.org/10.21203/rs.3.rs-9983173/v1

License: This work is licensed under a Creative Commons Attribution 4.0 International License.
Read Full License

Additional Declarations: No competing interests reported.

Glue-Free Femtosecond Laser Welding of Polymer–Glass Interfaces for Lab-on-Chip Devices

F. Torre*[a], M. Porta[a], A. Orlandini[a], F. Impaziente[a], A. Valente[a]

[a]Institute of Systems and Technologies for Sustainable Production (ISTePS), University of Applied Sciences and Arts of Southern Switzerland (SUPSI), via La Santa 1, 6962, Lugano, Switzerland

Abstract

Most micro laboratories, such as lab-on-chip (LOC), organ-on-a-chip (OoC), and microfluidics systems used in the biological sector, are made from materials such as glass, PMMA, and PDMS. These materials are chosen for their transparency, biocompatibility, and cost-effectiveness, despite each having unique properties and characteristics. Researchers have been motivated to combine different materials to leverage the advantages of each.

One process that enables the combination of substrates made from different materials is the ultrashort pulse (USP) welding process, which can be applied to transparent materials through femtosecond laser technology. A key advantage of this technology, compared to its classical counterpart, lies in its exploitation of non-linear absorption phenomena. This allows for localized energy deposition confined to the focal volume, resulting in a process that does not induce significant macroscopic thermal effects.

Unlike traditional methods, femtosecond laser welding eliminates the need for additional substances like adhesives or solders, enabling glue-free and solder-free joining of identical or different materials. This feature is especially beneficial in the fabrication of lab-on-chip devices, as it allows for the placement of biological substances without contaminating them.

The optimization of welding results involves analyzing the intensity distribution of absorbed energy at the materials interface and investigating the behaviour of the heat-affected zone (HAZ) under varying irradiation conditions.

This work aims to pave the way for new applications and results in the field of transparent material machining.

1. Introduction

Lab-on-chip (LOC) and organ-on-chip (OoC) devices play a crucial role in fields like pharmacology, immunology, and biochemistry [1]. These systems must fulfil two key criteria: they need to be biocompatible [2], to interact safely with biological samples, and optically transparent to enable imaging techniques such as fluorescence microscopy [3, 4].

Materials like PMMA and PDMS are widely used for their balance of biocompatibility, transparency, and affordability, making them common choices for LOC and OoC manufacturing platforms [5, 6].

On the other hand, glass offers excellent chemical stability, mechanical strength, and superior optical properties while also being inherently biocompatible [4]. In order to create precise hollow structures directly within glass, such as those suitable for LOC and OoC, the technique used is the Selective Laser Etching (SLE), a two step process involving femtosecond laser and wet chemical etching. A combination of this technique and ultrashort pulse (USP) laser welding allow the fabrication of micro laboratories

completely sealed in the inert glass, without requiring adhesives or additional components [7]. However, the high cost of SLE has led researchers to investigate alternative fabrication methods to manufacture such devices, such as soft lithography. In this approach, a mold is created (e.g., using SU-8 polymer), PDMS is poured into it, and then cured to form half of a chip [5]. These devices require a sealing step to complete the system, adding complexity to the process.

One of the least invasive sealing methods for microfluidic devices is USP laser welding. This technique directs a laser beam with a specific wavelength through transparent materials. At the focal point, nonlinear effects cause localized heating and phase transitions, melting the substrates together to form a strong bond [8].

This approach has been extended to different materials, such as PMMA and silicon (Si) wafers, as demonstrated by Capodacqua et al. [9]. They investigated how parameters like pulse energy, scanning speed, welding seams hatch distance, and repetition rate. The authors proposed a thermal model in which the laser radiation passes through the PMMA, to hit the silicon. Silicon is opaque and absorbs the light, causing its temperature to rise. This heat is then transferred back to the PMMA through conduction, causing it to melt and form a welded joint.

Volpe et al. [7] further explored how heat accumulation at rapid pulse intervals enhances the efficiency of the welding process. In the megahertz regime, pulses occur so quickly that there is no time for cooling between them, resulting in a continuous heat accumulation at the focal point, enabling more efficient melting. By optimizing these parameters, Volpe et al. minimized micro-explosions and voids, achieving a continuous melt zone and a robust welded joint.

When welding two substrates, the thermal expansion coefficients of the materials become a critical aspect, as significant differences can lead to cracks and defects. Zhang et al. [10] investigated the welding of SiC wafers and fused silica, materials with a melting point difference of over 1000°C. They achieved a welding seams with a tensile strength of 15.1 MPa, highlighting the crucial role of optical contact in significantly improving welding results and reducing the risk of ablation, which would otherwise consume energy needed for effectively melting the substrate. While clamping structures is often employed to ensure this condition, it can introduce internal stress in the material, potentially affecting the overall quality of the weld.

Cvecek et al. [11] investigated the behaviour of the melted zone in different types of glass substrates, performing welds between substrates with gaps as small as 1 µm. Their findings support the theory that the temperatures within the focal volume are sufficient to generate thermal expansion, causing the surface to bulge and fill the gap between the two substrates. During the cooling process, the bulged area contracts, exerting a pulling force on the joining substrates, thereby reducing or eliminating the gap.

These works aim to define the interaction between femtosecond lasers and transparent materials, studying the heat-affected zone and the required samples conditions, with the goal of applying these findings to optimize the welding process between polymers and glass.

2. Materials and methodology

2.1 Equipment

The laser system used for the experiments was the Femtika NanoFactory, a commercially available femtosecond laser workstation designed for advanced micromachining applications. This system utilizes a femtosecond laser based on chirped pulse amplification (CPA) and provides high beam

quality, with an M^2 factor of approximately 1.2. For this study, the laser operated at a wavelength of 1030 nm and offered tunable pulse durations ranging from 225 fs to 10 ps, with repetition rates between 60 kHz and 1 MHz. The maximum average power deliverable by the system is 4 W, and the scanning speed can reach up to 15 mm/s. The workstation is equipped with three objectives with varying magnifications, enabling flexible and precise microfabrication. For this work, the 10X objective was employed.

The Keyence® VHX-3000 is an optical microscope employed for detailed surface characterization and topographic analysis. It enables high-resolution imaging and quantitative measurements of surface roughness, providing vertical resolution (Z-accuracy) up to 0.2 µm and lateral resolution (XY-accuracy) up to 0.11 µm/pixel, depending on the objective lens and settings used. The system is particularly effective for comparing surface modifications under different laser processing parameters, offering both qualitative visualization and quantitative data acquisition.

2.2 Material

Material selection was guided by specific requirements of the biological experimental setup for studies on cells, as the commonly used PDMS is not very suitable for imaging and more prone to contamination when exposed to certain chemicals [12,13,14,15]. PMMA, on the other hand, is one good alternative material, due to its combination of optical transparency, biocompatibility, and oxygen permeability [16]. These properties ensure a high level of tissue tolerability, which supports the maintenance of the natural cell cycle and helps achieve reliable experimental outcomes by minimizing adverse reactions with the substrate. Furthermore, its good mechanical strength not only enhances the stability and durability of microfluidic devices but also ensures the maintenance of their shape under conditions that might otherwise cause structural deformation, such as significant pressure changes. This property minimizes the risk of flow inconsistencies, which are often observed in softer materials like PDMS, prone to deformation under high liquid pressures. [17]

Although PMMA provides excellent transparency, it is still not ideal for highly sensitive measurements due to its fluorescence [18]. In such instances', fused silica is chosen for its transparency and lower autofluorescence which is essential for accurately observing biological processes through the LOC surface [19]. Furthermore, glass typically has a finer surface finish than PMMA, which is processed via injection molding when used for LOC manufacturing, a process that can introduce bubbles, surface defects, and irregularities [20]. This difference in surface quality leads to less light scattering and improved resolution during microscopic analysis [21].

In fact, a good alternative to polymers is silica and borosilicate glass. The latter is a popular choice for manufacture LOC and OoC, particularly when the material's thermal stability and resistance to thermal shock are critical. Borosilicate glass is often preferred in microfluidic devices that require the ability to withstand high temperature gradients [22], such as those encountered during laser-based welding or thermal cycling during biological tests. The lower thermal expansion coefficient of borosilicate compared to PMMA makes it more stable under fluctuating temperatures, preventing stress and cracks in microfluidic channels. This characteristic is especially important when precise control over fluid dynamics and temperature-sensitive reactions is required. Furthermore, borosilicate glass combines good optical transparency with low fluorescence, making it suitable for high-precision optical measurements without compromising the quality of data collected during cell studies [23].

In our experiments, we adopted a commonly used borosilicate, Schott B270 [24], which is a type of high-quality borosilicate glass, widely used in precision applications (imaging, microscope slides) due to its excellent optical clarity, chemical resistance, and thermal stability.

2.3 Sample preparation

This study focuses on the development and application of devices made by PMMA and borosilicate glass.

The PMMA samples measured 25 mm in width and 43 mm in length. Each device featured eight large rectangular through-holes measuring 0.6 and 1 mm, interspersed with four smaller holes that were not considered. The welding process was designed to seal one face of the PMMA, effectively turning the larger through-holes into closed reservoirs/wells.

The glass samples used in this study were standard borosilicate microscope slides, with dimensions of 24 mm in width and 40 mm in length, and 0.13-0.16 mm in thickness.

Surface preparation was critical for ensuring successful welding. The PMMA surfaces were treated with 5000-grit sandpaper to achieve uniform opacity, while the glass samples were precisely cut to match the dimensions of the sealing area, corresponding to each through-holes In order not to have crack during the cells study at 37 °C we decided to decrease the area of each glass for thermal expansion reasons. To enhance weld quality, the glass surfaces underwent laser ablation to create a patterned area where the weld was planned. This pattern consisted of concentric rectangular geometries spaced 70 µm apart. The laser operated at 300 mW power, with a repetition rate of 200 kHz, a pulse duration of 225 fs and a scanning speed of 10 mm/s.

Prior to assembly, all surfaces were carefully cleaned to remove dust and ensure the closest possible distance between the PMMA and glass. Once positioned on the PMMA substrate, the glass samples were aligned over the respective holes. The assembled samples were then placed in the femtosecond workstation to perform the welding process.

3. Laser matter interaction

The laser parameters that have been used throughout our experiments are in the range that sees multiphoton-ionization regime dominate the laser-material interaction [25]. We therefore considered most of the energy that enabled material bonding coming from non-linear phenomena between the fs/ps laser pulses and the materials involved.

Material	Electron density (e/cm^3)	Band gap (eV)
Fused silica	~2.2×10^{23}	~9
PMMA	~3.2×10^{22}	4.273 [26]
Borosilicate D263	~2.2×10^{23}	~4.7

Given the material properties as listed above, the different capabilities to trigger nonlinear absorption, and the difference in thickness of the samples (the PMMA sample being much thicker compared to the glass), the experiment has been set to have the laser reaching the glass-PMMA interface passing through the glass. A defocus value between 0 and 50µm have been applied in order to maximize PMMA heating whilst reducing cracking at the glass interface. We then reversed the approach used by Capodaqua et al. [2], and avoided the heat transmission component from the glass to the PMMA, by having most laser absorption occur within the PMMA. This way it has been possible to operate at lower repetition rates (200kHz) and achieve clean bonding. In our observations, the key parameter for a solid

bond between glass and PMMA has been the total fluence at the glass-PMMA interface, that in turn relates to the amount of energy dissipated in the material.

A schematic description of the process can be deduced via the following equations. Laser spot size inside the medium can be expressed as:

$$\omega_0 = \frac{M^2 \lambda}{\pi NA} \tag{1}$$

In which M^2 is the laser beam parameter (≈ 1.2 in our setup), λ is the laser wavelength and NA is the numerical aperture of the setup.

When considering a defocus from the glass-PMMA interface, we used this formula to calculate the beam size at the interface, in which d_{Def} is the defocus and λ is the wavelength:

$$\omega_i = \omega_0 \sqrt{1 + \left(\frac{d_{Def}\, \lambda}{\pi \cdot \omega_0^2}\right)^2} \tag{2}$$

Using this beam size at the interface, the fluence was calculated classically using the following equation:

$$F = \frac{E_p N_p}{\pi \omega_i^2} \tag{3}$$

In which E_p is the pulse energy and N_p is the number of pulses for each point of the laser path, defined as

$$N_p = \frac{f \cdot \omega_i}{v} \tag{4}$$

For a fast processing and a clean bonding, we needed the laser to generate a wide band of molten PMMA around the laser track, as shown in Figure 2. We understood that optimal width (W_{melt}) for the molten region at the interface should be 100 μm or more. Considering an isotropic heat dissipation within the material, the size (volume V_{melt}) of the molten region would consequently scale up proportionally to the defocus (d_{def}) of the laser from the glass/PMMA interface, according to the following equation:

$$V_{melt}[\mu m^3] = \frac{4\pi}{3}\left(W_{melt}^2 - d_{def}^2\right)^{3/2} \tag{5}$$

A rough evaluation of the energy required by the material to show viscoelastic properties can then be calculated simply using classical heat transfer-heat dissipation formula:

$$Q = (T_v - T_0) C_{PMMA} + 4\pi \kappa_{PMMA}(T)\left(W_{melt}^2 - d_{def}^2\right)^2 \frac{dT}{dx} \tag{6}$$

In which T_v is the viscoelastic temperature for PMMA (116°C), T_0 is the ambient temperature of the experiment, κ_{PMMA} the thermal conductivity of PMMA, function of the temperature [27].

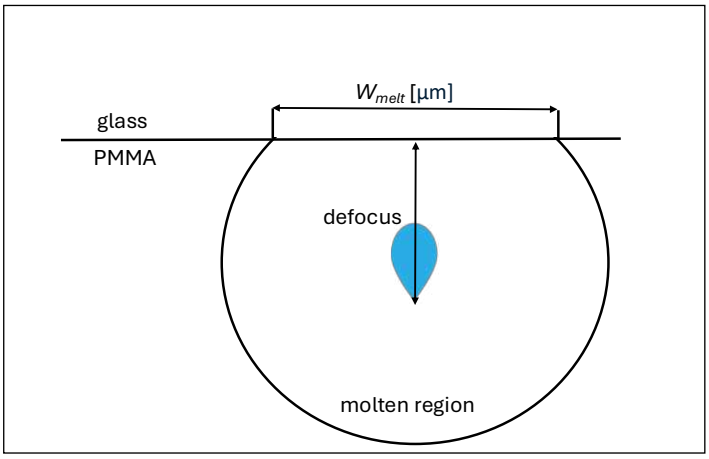


Figure 1 Schematic depiction of the section of the laser track, during the process of bonding.

This leads to a molten region volume that is proportional to the cube of the defocus. When matching the laser parameters and the material resistance to radiation and temperature generated by the laser interaction, the ideal defocus was found to be in the range of 30 to 40 µm. Higher defocus requires higher fluence to obtain a large enough molten region, but that would lead to a material deterioration of the sample, as shown in Figure 2b. Too small defocus, on the other hand, makes it difficult to close the gap between the glass and the PMMA, thus failing to provide a solid weld [11].

The optimum parameters (that require minimal material contamination) are the ones that generate a big enough molten region, without burning the PMMA. Figure 2 shows two regimes that lead to the material to join, although only sample (a) gives no contamination to the sample.

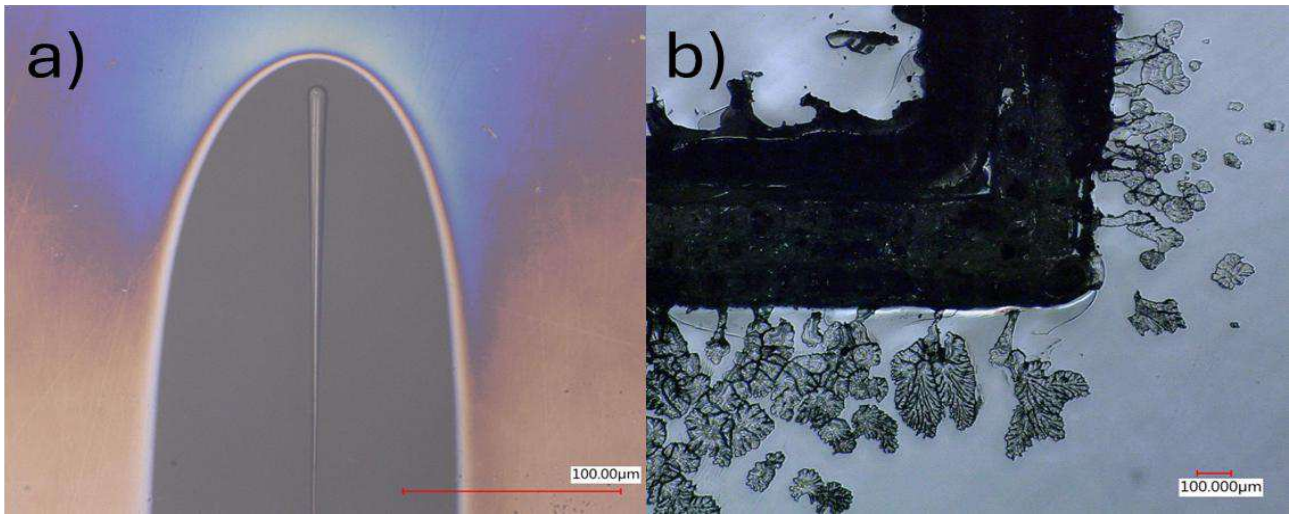


Figure 2 Optical images of two representative welding regimes. (a) Uniform molten region at the PMMA–borosilicate glass interface obtained under optimized processing conditions. (b) Weld obtained at higher energy input, showing material degradation at the interface.

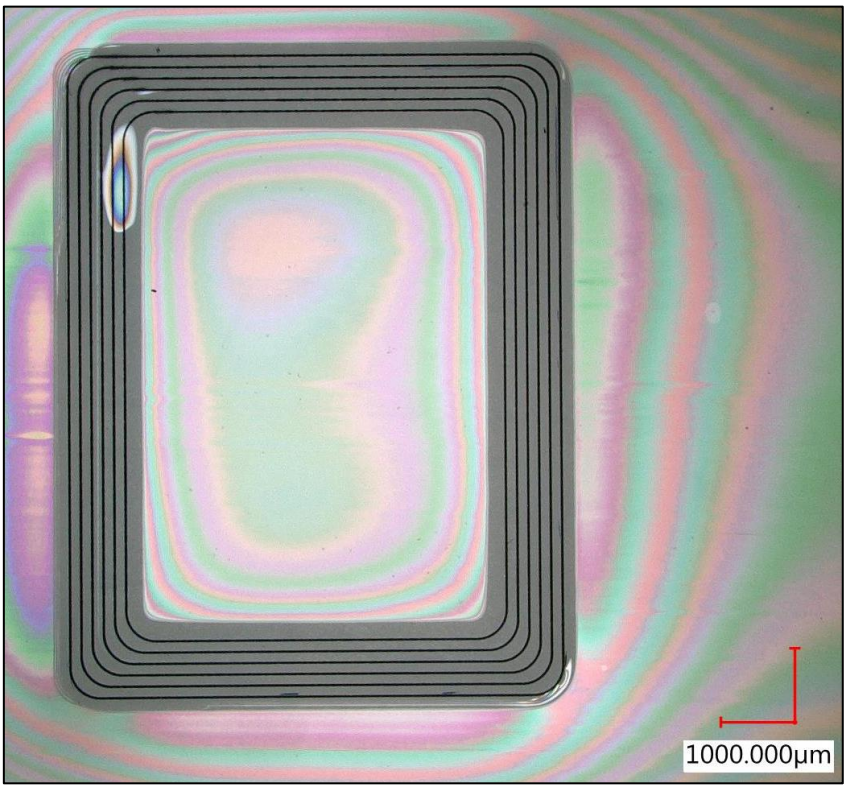


Figure 3 Microscope image of a laser-welded PMMA–borosilicate glass interface. A localized defect is visible in the upper-left region of the weld seam.

4. Results and discussion

4.1 Achieved Objective: Successful Fabrication and Durability of Welds

The goal of this study was to define laser welding parameters to perform strong and durable bonds between borosilicate and PMMA. Welds obtained under the optimized conditions were consistent. Visual inspection confirmed the homogeneity of the weld seam and showed no defects, such as bubbles, cracks, or surface damage (Figure 3). Mechanical testing further demonstrated that these bonds were reliable under applied stress. The tests were conducted using an H_2O-based marker inserted in the reservoirs formed by the glass–PMMA junction, maintained for 7 days at 37 °C.

The experimental results revealed important trends concerning the influence of various laser parameters on the quality of the bonding process. To investigate these effects systematically, some parameters were fixed—such as pulse duration and repetition rate—while others were varied, including laser power, pulse energy, and the distance between the focal point and the interface (defocus). A summary of the parameters used is shown in the table below.

Parameters fixed		Parameters varied
Pulse Duration	**Repetition Rate**	**Parameters Varied**
225 fs	200 kHz	• Pulse Energy:1.5-12.5 [µJ], • Scanning Speed: 0.35-1.6 [mm/s] • Defocus: 30-40 [µm]

4.2 Effect of Pulse Energy and Thermal Behaviour

Optimal welding in borosilicate was achieved with pulse energies between 2.25 µJ and 3 µJ; in Figure 4 is an example of a successful weld. The resulting heat-affected zone (HAZ) consistently displayed two distinct regions: a central darker zone corresponding to the laser impact area and a surrounding lighter region, both showing clear signs of melting and resolidification. The high thermal conductivity of borosilicate facilitated efficient thermal energy absorption and redistribution, promoting controlled heat diffusion and enabling the formation of well-defined welds. This thermal behaviour contributed to successful weld formation over a broad fluence range, making borosilicate resilient to process fluctuations.

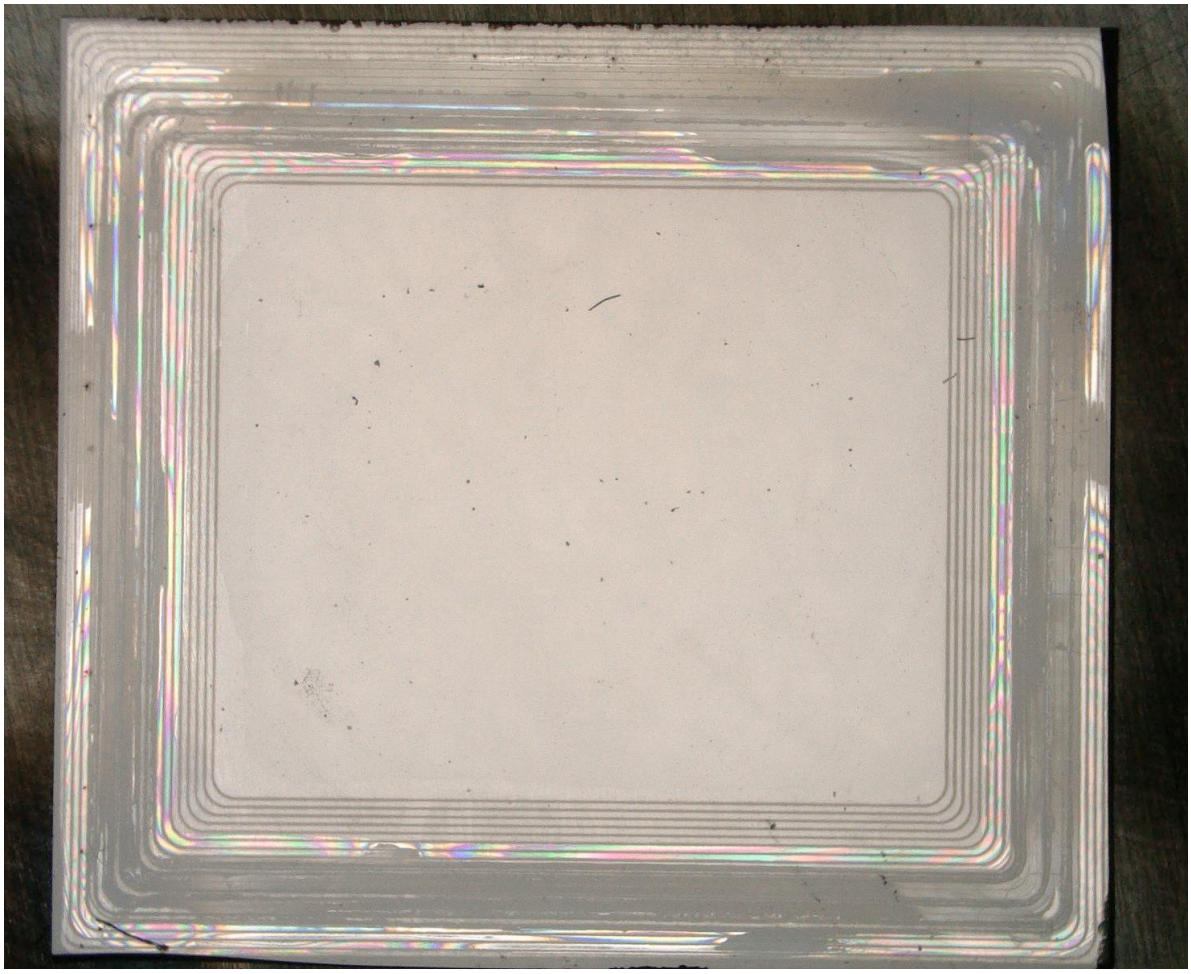


Figure 4 Heat-affected zone morphology at the borosilicate glass–PMMA interface under optimized pulse energy conditions.

4.3 Influence of Defocus on Weld Quality

The defocus parameter also played a crucial role in determining weld quality. A defocus between 30 and 40 µm generally produced optimal results, with a consistent, sharply defined HAZ showing evident melting and resolidification (Figure 6). At a defocus of 30 µm, the spot size was approximately 5.16 µm calculated using the formula (2). Further tests were performed with a defocus up to 50 µm, which revealed two main issues. First, the welds became excessively wide without achieving sufficient melting of the PMMA next to the glass interface to form a proper bond. Second, although the focal point was shifted away from the glass surface, the higher power required to have the melt reach the glass-PMMA interface caused a disruption in the process, resulting in contamination at the interface and ultimately compromising the process.

4.4 Effect of Laser Power

From tested parameters emerged that increasing the power, from 300mW to 1000mw, led to a more homogeneous fused areas. Notably, welds from 450 mW to 600 mW exhibited extensive and uniform central dark zones, indicating improved material coupling and melt continuity. However, at the highest tested power, 2500 mW, signs of overextended HAZ and seam irregularities began to emerge (Figure 7 a) is an example of damaged sample), suggesting a practical upper limit for stable processing.

Figure X summarizes the effect of laser power and scanning speed on the quality of the PMMA–borosilicate glass welds. At low scanning speeds, increasing laser power led to higher energy deposition, resulting in wider weld seams but also an increased risk of thermal damage. Conversely, higher scanning speeds required greater laser power to achieve sufficient interfacial melting, defining a narrow process window for defect-free welding. Optimal welding conditions were identified in the intermediate power–speed region, where stable bonding was achieved without visible burns or cracks.

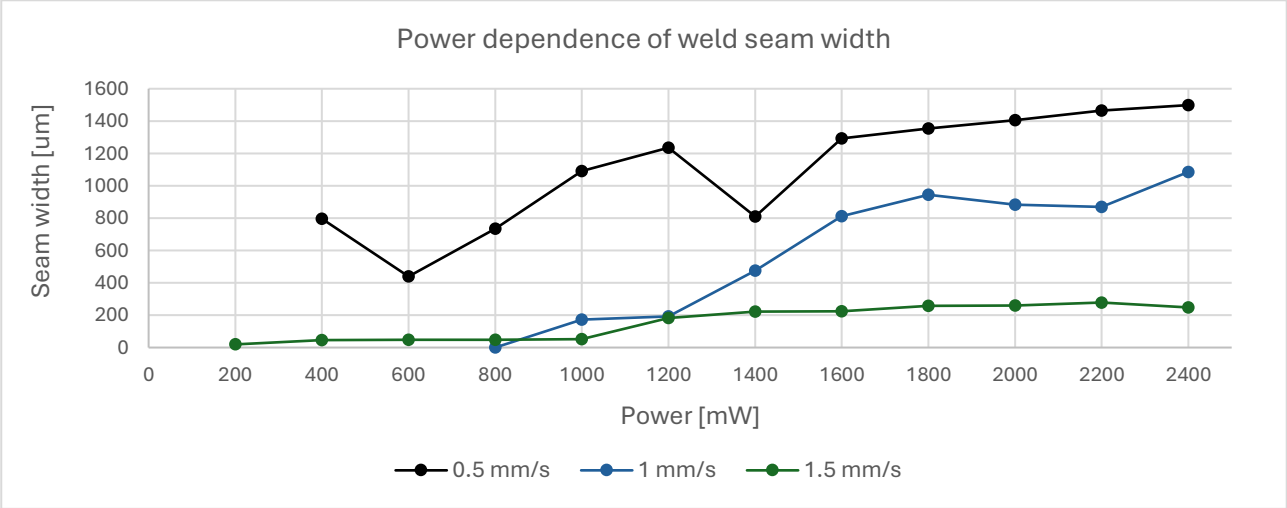


Figure 5 Process map showing the combined effect of laser power and scanning speed on PMMA–borosilicate glass welding quality.

4.5 Effect of cumulative fluence

In addition to individual laser parameters, cumulative fluence — which considers the combined effect of pulse energy, repetition rate, and scanning speed — was found to be a reliable predictor of weld stability. Cumulative fluence values around 9.5E+03 ensured sufficient thermal accumulation for melting while avoiding overheating or excessive HAZ extension. Also, higher values of fluence ensure the sealing between samples, with fluence values around 5E+04 J/cm^2. Still, these compromise the optical clarity and the purity of the samples due to damage induced by heat accumulation. Figure 7 shows three different behaviours that could lead to a good weld, but the results differ in terms of clarity and purity.

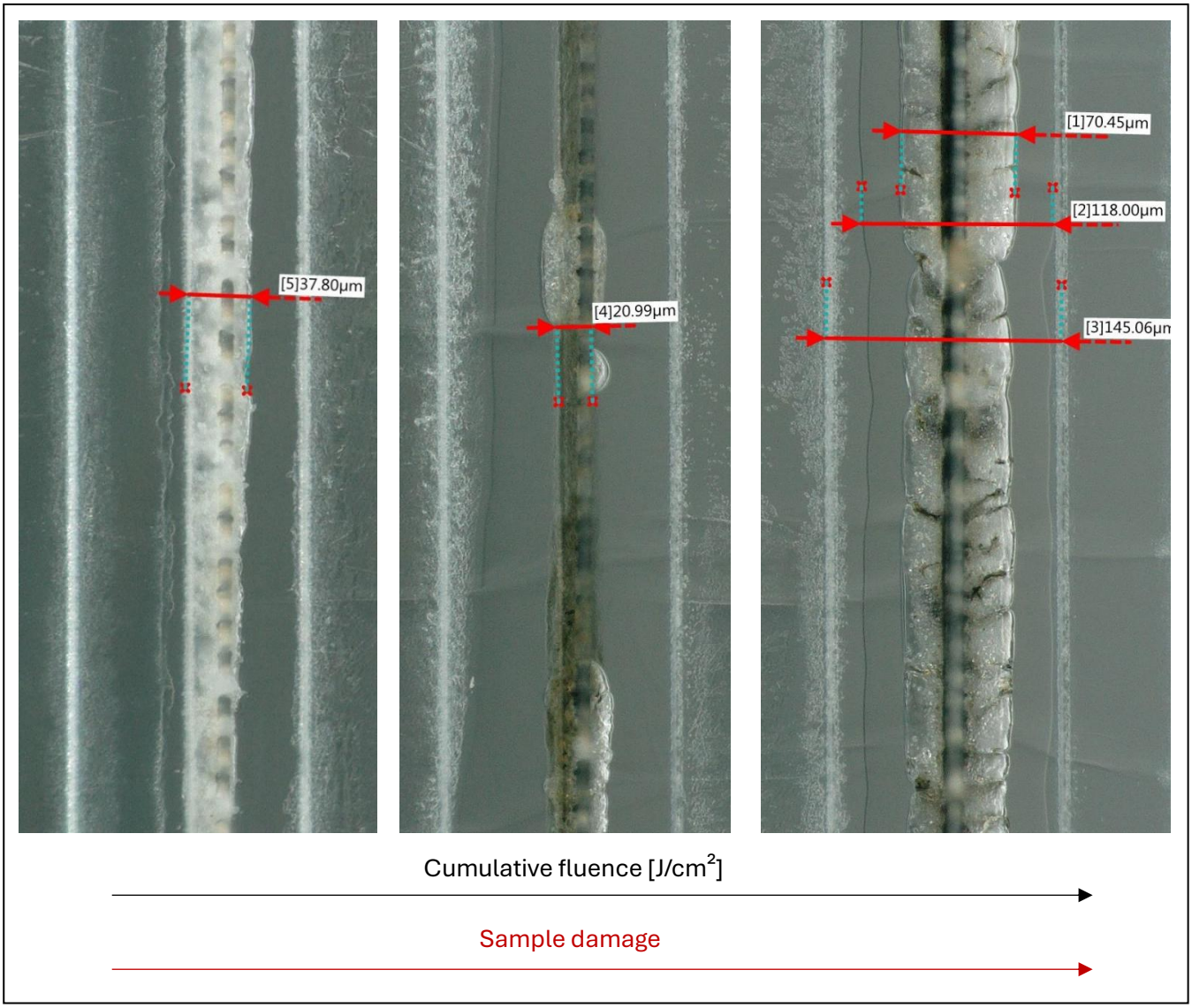


Figure 6 Representative microscope images of laser-welded PMMA–borosilicate glass interfaces obtained at different cumulative fluence values, showing distinct weld morphologies and heat-affected zone extensions.

4.6 Effect of cumulative fluence

For a fixed pulse energy and repetition rate, a higher scanning speed leads to a decrease in cumulative fluence. This enhanced melt pool uniformity and bonding strength. This was particularly evident when comparing welds performed at 0.35 mm/s and 1.0mm/s under identical power and defocus conditions

(see Figure 7). At lower speeds, the higher cumulative fluence resulted in damage due to heat accumulation and occasional incomplete bonding, while higher speeds provided optimal energy deposition for consistent, defect-free seams.

To address minor inconsistencies, the scanning speed was progressively reduced by 20% to 80% near sharp corners and track ends, effectively minimizing abrupt changes in direction and improving seam continuity.

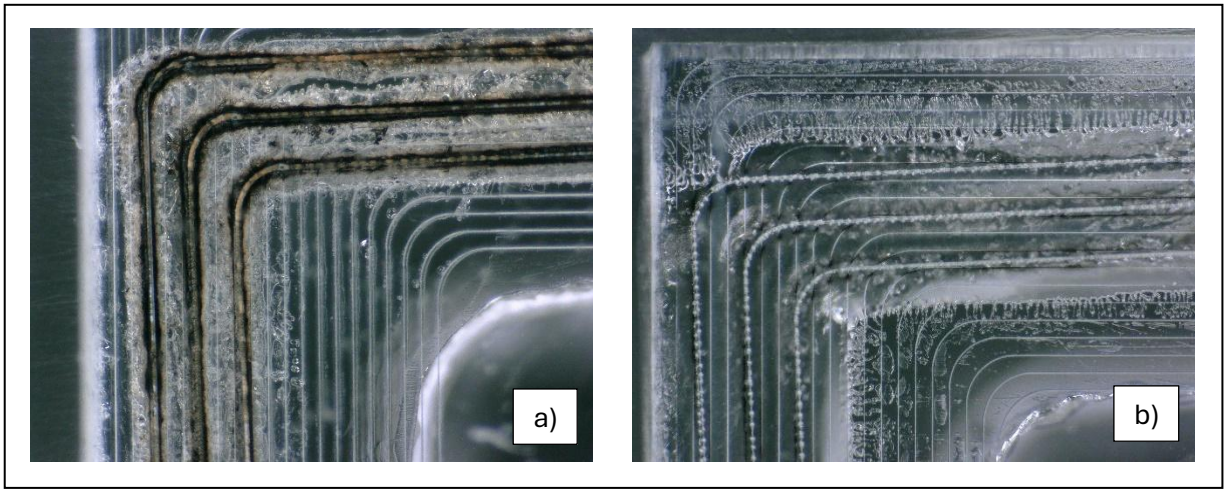


Figure 7 Microscope images of laser-welded PMMA–borosilicate glass interfaces obtained at different scanning speeds under identical pulse energy, repetition rate, and defocus conditions: (a) 0.35 mm/s and (b) 1.0 mm/s.

5. Conclusions

This study demonstrates that femtosecond laser welding is an effective method for bonding borosilicate glass to PMMA, provided that process parameters are carefully optimized to avoid thermal degradation. The primary objective was to achieve contamination-free welds with reliable mechanical integrity. Although some samples exhibited sufficient adhesion, any signs of burning or material degradation rendered them unsuitable for applications requiring optical clarity and biocompatibility.

To ensure a robust and uniform weld seam, a defocus of 40 µm was identified as optimal. This configuration allowed for increased laser power without inducing thermal damage laying under the damage threshold, enabling the formation of a sufficiently wide molten region at the interface. The ability to expand the weld line without compromising material integrity was critical to achieving high-quality results.

Experimental evidence confirmed that cumulative fluence is a key predictor of weld performance. Values around 9.5E+03 J/cm^2 consistently produced stable, defect-free bonds. Higher fluence levels (up to 4.93E+04 J/cm^2) also exhibit good mechanical strength, but cause material defect formation.

Leakage tests on Petri-dish–like devices were conducted by filling each chamber with a coloured aqueous solution and monitoring them for 7 days, as shown in Figure 8. The highlighted areas in the image correspond to the samples that exhibited the best performance after 7 days, showing no evidence of cracks, leakage, or thermal damage.

In summary, successful welding between PMMA and borosilicate glass requires a balance between energy delivery and thermal management. The process window defined by defocus, scanning speed, and cumulative fluence enables the formation of strong, clean welds suitable for microfluidic and biological applications, without the need for adhesives or intermediate layers.

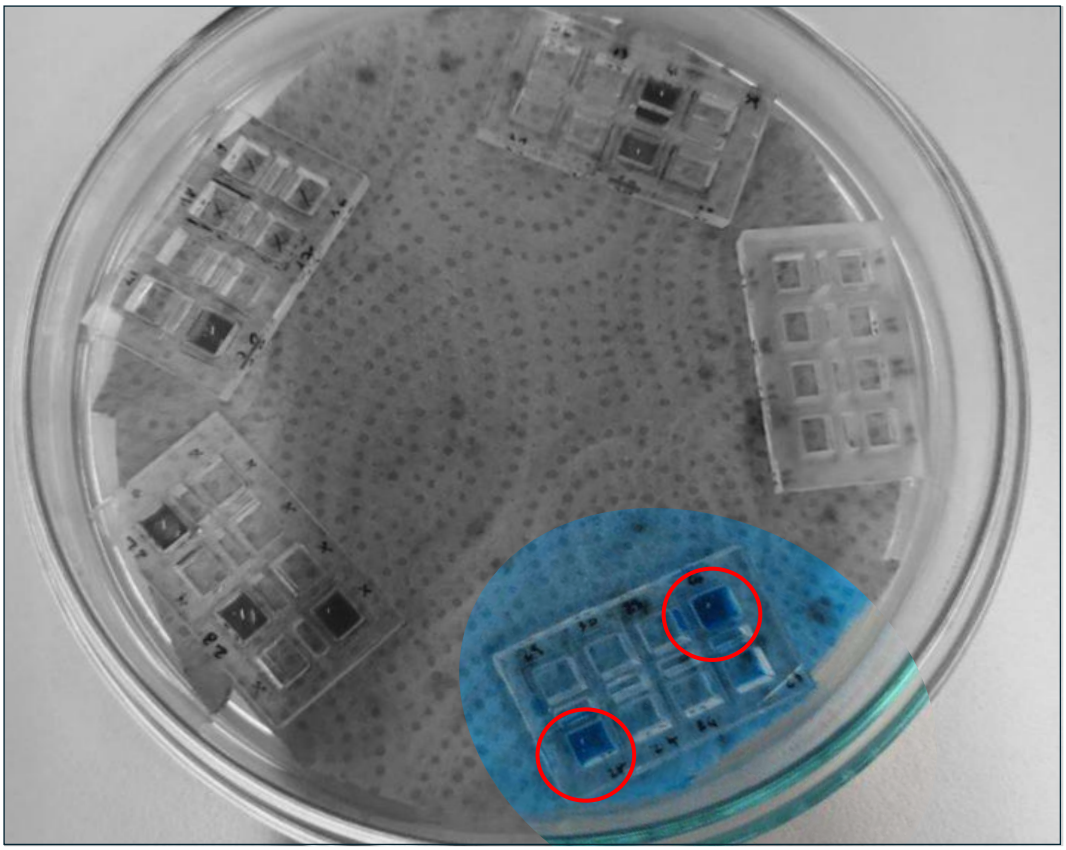


Figure 8 Leakage test on Petri-dish–like devices filled with a coloured aqueous solution and monitored for 7 days. Highlighted samples show no cracks, leakage, or thermal damage after the test period.

Declarations

Ethical Approval

Not applicable. This study did not involve human participants, human data, or animals.

Funding

This work has been supported by the WISE project – Multi-scale multi-process machine for high value-added complex products with disruptive functionalities, funded by the Horizon Europe research and innovation programme under Grant Agreement No. 101138718.

Availability of data and materials

The datasets generated and/or analysed during the current study are available from the corresponding author upon reasonable request.

References

[1] N. Farhang Doost and S. K. Srivastava, “A Comprehensive Review of Organ-on-a-Chip Technology and Its Applications,” *Biosensors*, vol. 14, art. 225, 2024.

[2] H. Zhang, J. Wang, and Y. Liu, “Biomedical Application of Functional Materials in Organ-on-a-Chip,” *Advanced Functional Materials*, vol. 30, art. 2002041, 2020.

[3] Y. Zheng, Y. Chen, J. Chen, et al., “Lab-on-a-chip technologies for stem cell research,” *Micromachines*, vol. 11, art. 361, 2020.

[4] C. M. Dixit, P. S. Bhat, and R. Prabhakar, “The autofluorescence of plastic materials and microfluidic chips under laser excitation,” *Lab on a Chip*, vol. 18, pp. 357–365, 2018.

[5] M. Madou, “Injection molded lab-on-a-disc platform for screening applications,” *Lab on a Chip*, vol. 14, pp. 361–374, 2014.

[6] A. R. Hassan, M. M. Khan, and P. S. Yadav, “Low-cost inertial microfluidic device for microparticle separation: a laser-ablated PMMA lab-on-a-chip approach without a cleanroom,” *Microsystems & Nanoengineering*, vol. 6, art. 92, 2020.

[7] A. Volpe, P. Paiè, A. Ancona, and R. Osellame, “Ultrafast laser bonding of glasses and crystals to metals for epoxy-free optical instruments,” *Optics Express*, vol. 23, pp. 4114–4126, 2015.

[8] K. Sugioka and Y. Cheng, “Internal modification of glass by ultrashort laser pulses,” *Applied Physics Reviews*, vol. 1, art. 041303, 2014.

[9] M. Capodacqua, P. Paiè, A. Ancona, and R. Osellame, “Femtosecond laser welding of PMMA to silicon,” *Optics Letters*, vol. 43, pp. 331–334, 2018.

[10] Y. Zhang, X. Wang, and J. Li, “Interface modification based ultrashort laser microwelding between SiC and fused silica,” *Optics and Lasers in Engineering*, vol. 121, pp. 1–7, 2019.

[11] K. Cvecek, I. Miyamoto, and M. Schmidt, “Gap bridging in joining of glass using ultrashort laser pulses,” *Optics Express*, vol. 26, pp. 878–889, 2018.

[12] Y. Ma, P. Zhou, H. Wang, and Y. Mao, “Thermal effect on poly(methyl methacrylate) material removal in the micromilling process,” *Polymers*, vol. 12, art. 2122, 2020.

[13] E. Sackmann, A. Fulton, and D. Beebe, “The present and future role of microfluidics in biomedical research,” *Nature*, vol. 507, pp. 181–189, 2014.

[14] E. Primiceri, M. S. Chiriacò, R. Rinaldi, and G. Maruccio, “Cell chips as new tools for cell biology: results, perspectives and opportunities,” *Lab on a Chip*, vol. 13, pp. 378–391, 2013.

[15] A. Volpe, P. Paiè, A. Ancona, and R. Osellame, “Polymeric fully inertial lab-on-a-chip with enhanced-throughput sorting capabilities,” *Microfluidics and Nanofluidics*, vol. 23, art. 37, 2019.

[16] X. Ma, R. Li, Z. Jin, et al., “Injection molding and characterization of PMMA-based microfluidic devices,” *Microsystem Technologies*, vol. 26, pp. 1317–1324, 2020.

[17] B. Nguyen and D. Papautsky, “Flow rate–pressure drop relationships in microfluidic channels,” *Microfluidics and Nanofluidics*, vol. 8, pp. 193–210, 2010.

[18] J. R. Lakowicz, “Autofluorescence Detection in Analytical Chemistry and Biochemistry,” *Analytical Biochemistry*, vol. 298, pp. 1–24, 2001.

[19] Y. Chen, Y. Zhang, L. Liu, et al., “A simple and reversible glass–glass bonding method to construct a microfluidic device and its application for cell recovery,” *Lab on a Chip*, vol. 12, pp. 4373–4381, 2012.

[20] X. Liu, A. Sun, J. Brodský, et al., “Microfluidics chips fabrication techniques comparison,” *Scientific Reports*, vol. 14, art. 28793, 2024.

[21] S. Shelby, T. R. Shrout, and J. M. Ihlefeld, “Thermal and mechanical characterization of borosilicate glass,” *Journal of the American Ceramic Society*, vol. 98, pp. 255–262, 2015.

[22] A. O. Ståhlberg, M. A. Nilsson, and S. P. Eriksson, “Electrokinetic delivery of single fluorescent biomolecules in fluidic nanochannels,” *Nano Letters*, vol. 15, pp. 215–220, 2015.

[23] SCHOTT AG, “B 270® Thin borosilicate glass – Material Data Sheet,” SCHOTT, 2022.

[24] B. Rethfeld, “Free-electron generation in laser-irradiated dielectrics,” *Physical Review B*, vol. 73, art. 035101, 2006.

[25] Q. M. Al-Bataineh, A. A. Ahmad, A. M. Alsaad, and A. D. Telfah, “Optical characterizations of PMMA/metal oxide nanoparticles thin films,” *Heliyon*, vol. 7, art. e05952, 2021.

[26] V. Mathur and K. Sharma, “Thermal response of polystyrene/poly(methyl methacrylate) polymeric blends,” *Heat and Mass Transfer*, vol. 52, pp. 1565–1576, 2016.

[27] X. Liu, A. Sun, J. Brodský, et al., “Microfluidics chips fabrication techniques comparison,” *Scientific Reports*, vol. 14, art. 28793, 2024.